Transition from damage to fragmentation in collision of solids

Ferenc Kun[1,2,*] and Hans J. Herrmann[1]
[1]*Institute for Computer Applications (ICA1), University of Stuttgart, Pfaffenwaldring 27, D-70569 Stuttgart, Germany*
[2]*Department of Theoretical Physics, Kossuth Lajos University, P.O. Box 5, H-4010 Debrecen, Hungary*
(Received 17 September 1998)

We investigate fracture and fragmentation of solids due to impact at low energies using a two-dimensional dynamical model of granular solids. Simulating collisions of two solid disks, we show that, depending on the initial energy, the outcome of a collision process can be classified into two states: a damaged state and a fragmented state, with a sharp transition in between. We give numerical evidence that the transition point between the two states behaves as a critical point, and we discuss the possible mechanism of the transition. [S1063-651X(99)15302-9]

PACS number(s): 64.60.Ak, 46.50.+a

I. INTRODUCTION

Fragmentation, i.e., the breaking of particulate materials into smaller pieces, is a ubiquitous process that underlies many natural phenomena and industrial processes. The length scales involved in it range from the collisional evolution of asteroids through the scale of geological phenomena down to the breakup of heavy nuclei [1,2]. In most of the realizations of fragmentation processes the energy is imparted to the system by impact; i.e., typical experimental situations are shooting a projectile into a solid block, free fall impact with a massive plate, and collision of particles of the same size [3–11]. The most striking observation about fragmentation is that the size distribution of fragments shows a power law behavior independent of the microscopic interactions and the relevant length scales; e.g., the charge distribution of small nuclei resulted from collisions of heavy ions exhibits the same power law behavior as the size distribution of asteroids [1–11]. Experiments revealed that the power law behavior of fragment sizes is valid for a broad interval of the imparted energy [3–11], which was also reproduced by computer simulation of sophisticated microscopic models [12–17]. The observation of power law size distributions without a control parameter initiated the idea of self-organized criticality [8–11,18,19] in fragmentation, and gave rise to numerous studies to understand the dynamic origin of the power law [12–25]. Hence during the past years much information has been accumulated about fragmentation processes in the imparted energy range where a power law size distribution occurs, but the limiting case of low energies is still not explored.

In addition to the general interest in fragmentation processes, one can also mention other fields where fracture and fragmentation of solid particles due to impact play an important role. It is well known that in the flow of granular materials a large part of the kinetic energy of the grains is dissipated in the vicinity of their contact zone during the collisions. In addition to the viscous and plastic effects, dissipation by damaging is also an important source of energy loss in the flow. Collision of particles also occurs in the solar system in planetary rings. In this case the energy dissipation due to impact damage might also influence the large scale structure formation in the rings [26]. On a larger length scale in the solar system, the so-called collisional evolution of asteroids due to subsequent collisions, and the formation of rubble piles in the asteroid belt, are still challenging problems [6]. Among industrial applications the breakup of agglomerates in chemical processes can be mentioned. Due to experimental difficulties, the computer simulation of microscopic models is an indispensable tool in the study of these impact phenomena [12–17].

In the present paper we want to elaborate upon the impact fracture and fragmentation of solids at low imparted energy using a two-dimensional dynamical model of breakable granular solids. Simulating collisions of two solid disks, we show that, depending on the imparted energy, the outcome of a collision process can be classified into two states: a damaged state and a fragmented state, with a sharp transition in between. Analyzing the energetics of the impact and the resulting fragment size distributions, we give numerical evidence that the transition point between the damaged and fragmented states behaves as a critical point. The transition proved to be the lower bound for the occurrence of power law size distributions. The possible mechanism of the transition between the two states is discussed. In spite of the specific features of the system studied here, most of our results can be considered generally valid for impact phenomena mentioned above.

After giving a short summary of the main ingredients of our model in Sec. II, the numerical results concerning to the energetics of the collision process and to the size distribution of fragments will be presented in Secs. III and IV, respectively. In Sec. V, we discuss the possible mechanism of the transition and some general consequences of our work for other types of fragmentation phenomena.

II. MODEL

Recently, we have worked out a two-dimensional dynamical model of deformable, breakable, granular solids, which enables us to perform a molecular dynamics simulation of

*Electronic address: feri@ica1.uni-stuttgart.de

 ©1999 The American Physical Society

fracture and fragmentation of solids in various experimental situations [12,13]. Our model is an extension of those models which are used to study the behavior of granular materials, applying randomly shaped convex polygons to describe grains [27]. To capture the elastic behavior of solids we connect the unbreakable, undeformable, polygons (grains) by elastic beams. The beams, modeling cohesive forces between grains, can be broken according to a physical breaking rule, which takes into account the stretching and bending of the connections. The breaking rule contains two parameters t_ϵ and t_Θ controlling the relative importance of the stretching and bending breaking modes, respectively. The energy stored in a beam just before breaking is released in the breakage, giving rise to energy dissipation. The average value of the energy dissipated by the breakup of one contact defines the crack surface energy E_s in the model solid as a function of the breaking parameters t_ϵ and t_Θ. At the broken beams along the surface of the polygons, cracks are generated inside the solid, and as a result of the successive beam breaking the solid falls apart. The fragments are defined as sets of polygons connected by remaining intact beams. In the framework of this discrete model one can introduce the notion of the binding energy E_b as the energy released in the case of complete disintegration, i.e., in the case when all the fragments are single polygons. Hence,

$$E_b = N_c E_s, \tag{1}$$

where N_c denotes the total number of grain-grain contacts in the solid. Note that E_b is proportional to the volume of the sample, and can be considered as a natural energy scale of the system.

The time evolution of the fragmenting solid is obtained by solving the equations of motion of the individual polygons until the entire system relaxes, i.e., there is no breaking of the beams during some hundreds of consecutive time steps, and there is no energy stored in deformation. For more details of the model's definition, see Refs. [12,13].

We have applied the model to study shock fragmentation of solids in various experimental situations. That is, simulations were performed to study the fragmentation of a solid disk caused by an explosion in the middle [12], the breaking of a rectangular block due to the impact with a projectile [12], and the collision of two macroscopic bodies (disks) [13]. The model proved to be successful in reproducing the experimentally observed subtleties of fragmenting systems, e.g., the power law mass distribution of fragments was found to be independent of the initial conditions, with an exponent in the vicinity of two, slightly depending on the initial energy [12,13].

III. DAMAGE AND FRAGMENTATION

In the present paper we apply our model to explore the properties of impact fragmentation processes at low imparted energy. For this purpose we carried out molecular dynamics simulation of the collision of two solid disks of the same size, similar to Ref. [13]. The disk-shaped granular solid was obtained starting from the Voronoi tessellation of a square [28,29], and cutting out a circular window in the middle. This way of construction gives rise to a certain surface roughness of the particles. The schematic representation of the collision of two particles is depicted in Fig. 1. For simplicity, in the present studies only central collisions were considered; i.e., the value of the impact parameter b was set to zero in all the simulations, and only the size of the particles R and the surface energy E_s were varied. In the simulations the energy release by beam breaking is the only possible source of dissipation. The energy of the collision E_0 is defined as the total initial kinetic energy of the colliding bodies,

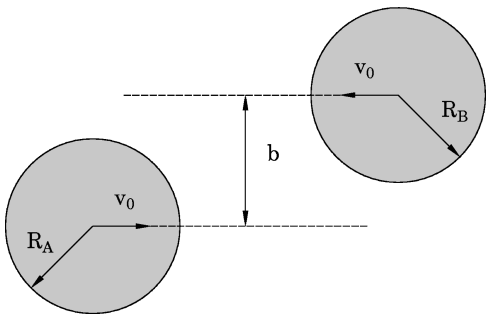

FIG. 1. The schematic representation of the collision of two disks. In all the simulations $R_A = R_B$ was used, and the value of b was set to 0.

$$E_0 = R^2 \pi \rho v_0^2, \tag{2}$$

where ρ is the mass density and v_0 denotes the initial velocity of the particles. When E_0 is smaller than the so-called damage threshold E_d, the collision results simply in elastic rebound without internal damage (without breaking of beams). To achieve damaging, E_0 has to surpass the damage threshold E_d, which is determined by the surface energy E_s of the model.

It is generally accepted that impact fragmentation phenomena exhibit so-called energy scaling, i.e., the result of the fragmentation process only depends on the value of the specific energy defined as the imparted energy divided by the total mass of the system. To characterize the collision events, we introduce a dimensionless parameter η with the definition

$$\eta = \sqrt{\frac{E_0}{E_b}} \sim \frac{v_0}{\sqrt{E_s}}. \tag{3}$$

This choice of parameter η has the advantage with respect to the specific energy that, besides the dependence on the global size, it also includes the specific material type through the surface energy E_s. Since in the present study we focus on the evolution of damage with increasing impact energy, simulations were performed at fixed values of R and E_s varying η in the range $\eta_0 < \eta < 1.5$. Here η_0 corresponds to the damage threshold $\eta_0 = \sqrt{E_d/E_b}$. Our results concerning impact fragmentation at $\eta > 1.5$ can be found in Ref. [13], including a detailed analysis of the dynamics of the collision process and a comparison to experiments. The values of the most important parameters of the present simulations are summarized in Table I.

In Fig. 2 we present the final breaking scenarios (relaxed states) of the collision process obtained by simulations at four different values of η. It can be observed that for $\eta \sim \eta_0$ [Fig. 2(a)], cracking by beam breaking occurs mainly

TABLE I. The parameter values used in the simulations.

Parameter	Symbol	Unit	Value
Failure elongation of a beam	t_ϵ	%	3
Failure bending of a beam	t_Θ	degree	4
Surface energy	E_s	erg	1.4×10^6
Damage threshold	E_d	erg	1.7×10^8
	η_0	1	0.08
Range of velocities	v_o	cm/s	200–3500

in the vicinity of the contact surface of the two bodies, and the bulk remains practically intact. Since this gentle collision does not cause size reduction of the two particles, this case can be considered as an inelastic impact of disks, where energy dissipation is solely due to internal damage. Increasing the impact energy E_0, i.e., increasing η, gives rise to more broken beams in Fig. 2(b), and the solids break into pieces. Around the impact site of the bodies the fragments are smaller (single polygons, and some pairs and triplets), and there are a few much larger fragments the size of which is still comparable to the original size of the bodies. Further increase of η [Figs. 2(c) and 2(d)] mainly results in a breakup of the large fragments into smaller ones, giving rise to fragmentation of the entire solids. Based on the above qualitative picture, we classify the outcome of a collision into two states, i.e., *damaged* and *fragmented* states, distinguished by the size of the largest remaining piece. The colliding bodies are considered to be *damaged* when the size of the largest piece is comparable to the original size of the bodies [see Figs. 2(a) and 2(b)], while the *fragmented* state is characterized by the absence of such large pieces [Figs. 2(c) and 2(d)]. In the following we point out that the above qualitative picture is also supported by a quantitative analysis of the energetics of the collision process and of the behavior of the resulting size distribution of fragments. That is, evaluating the energy released by the breaking of beams, and quantities related to the size distribution of fragments, we will justify that the behavior of the colliding system has two different regimes with a sharp transition in between.

The energetics of the collision process corresponding to the samples of Fig. 2 is summarized in Figs. 3 and 4. Figure 3 shows the energy E_R released by beam breaking, together with the remaining kinetic energy E_0-E_R stored in the motion of fragments as a function of η. For the purpose of comparison, the surface energy E_s of the model, the binding energy of the sample E_b, and the energy of the impact E_0 are also plotted in the figure. When the impact energy E_0 surpasses the damage threshold E_d (η surpasses η_0), the released energy E_R takes its smallest value, which is equal to the surface energy E_s of the model (only one beam is broken). The largest possible value of E_R is equal to the binding energy of the sample E_b, which can only be reached in the case of complete disintegration. According to the simulations, this limiting case is hard to achieve, since on the surface of the colliding disks opposite to the impact site, small fragments comprising a few polygons can always escape. It can also be seen in the figure that the impact energy E_0 producing complete disintegration has to be much larger than

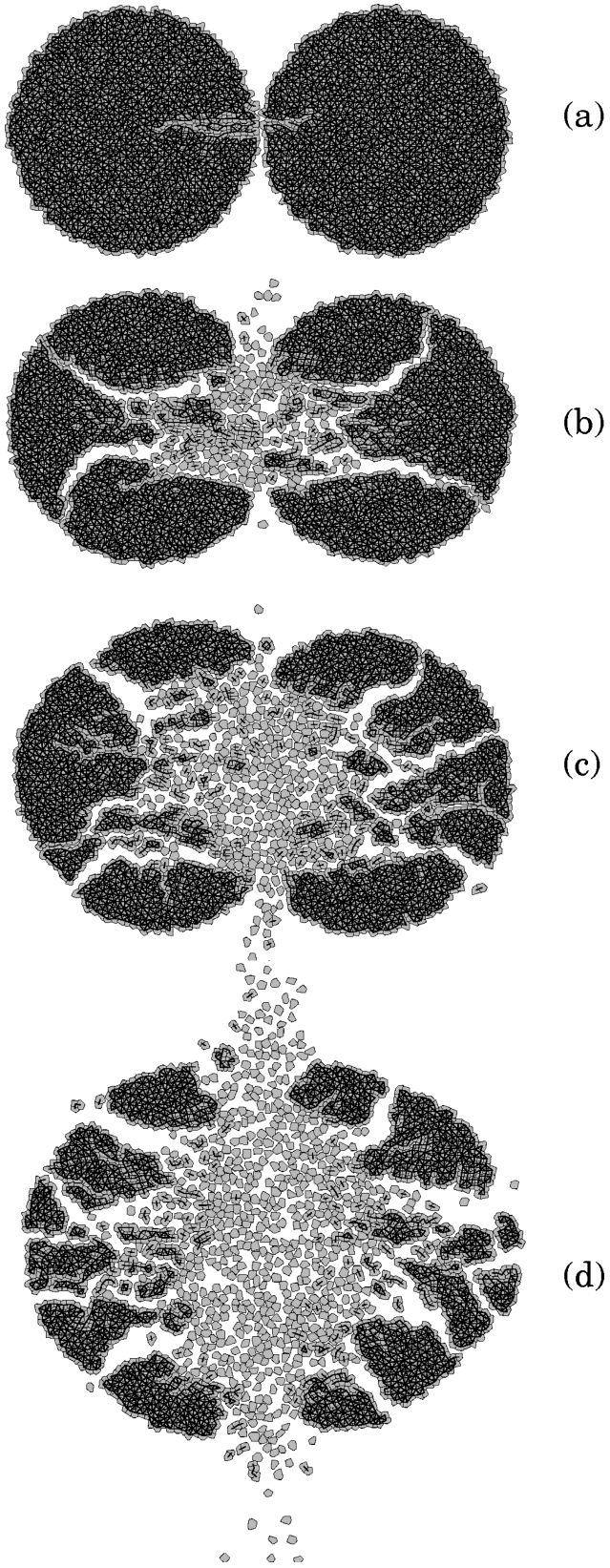

FIG. 2. The final breaking scenarios of collisions of disks at different impact energies E_0. The radius of the disks is $R=20$ cm, while the average size of a randomly shaped polygon is 1 cm. The lines connecting the center of mass of the neighboring polygons symbolize beams. The missing beams have already been broken. The values of the parameter η are 0.09, 0.2, 0.3, and 0.5 for (a), (b), (c), and (d), respectively.

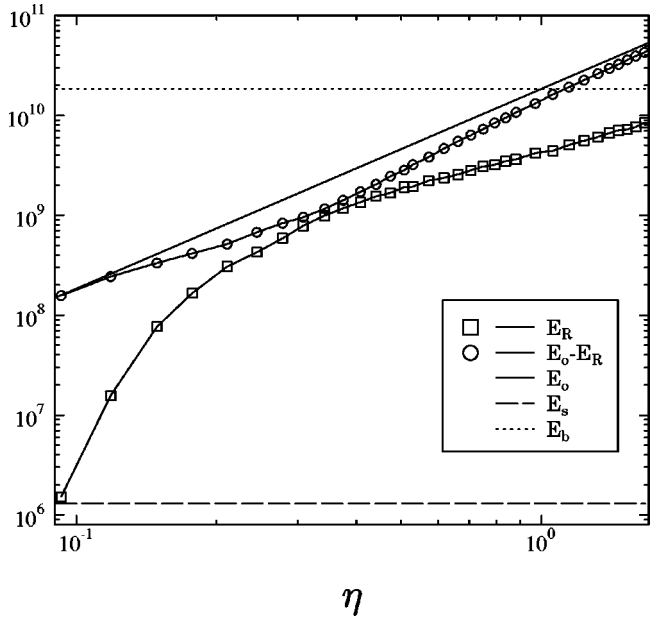

FIG. 3. The energy released by beam breaking E_R and the kinetic energy stored in the motion of fragments E_0-E_R. For comparison, the surface energy E_s of the model, the binding energy of the sample E_b, and the energy of the impact E_0 are also indicated. The energy unit is erg. For the exact values see Table I.

the binding energy E_b. Note that a similar qualitative behavior was found, simulating the free fall impact of a disk with a massive plate [16].

The most interesting observation of Fig. 3 is that the curve of E_R versus η is composed of two distinct parts; i.e., a rapidly increasing low energy part, and a slowly increasing high energy part. These two regimes are separated by a point where E_R is practically equal to the remaining kinetic energy E_0-E_R, which implies that at this point half of the total kinetic energy E_0 is released by cracking. The two regimes

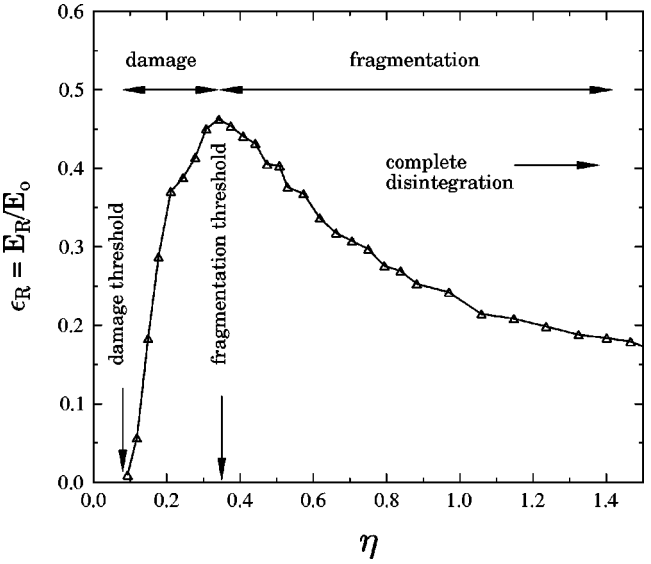

FIG. 4. The ratio ϵ_R of the energy released by breaking E_R and the total kinetic energy E_o. The transition point (fragmentation threshold) between the damaged and fragmented states is identified with the position of the maximum of ϵ_R.

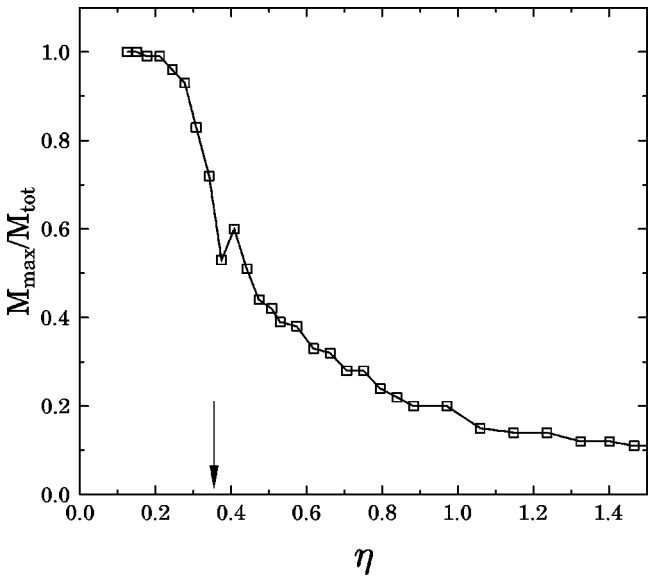

FIG. 5. The mass of the largest fragments divided by the total mass of the colliding system. The arrow indicates the fragmentation threshold η_c.

can be better observed in Fig. 4, where the ratio ϵ_R of E_R and E_0 is plotted against η. The curve of ϵ_R has a maximum, the value of which is in the vicinity of 0.5. This maximum separates a rapidly increasing part and a slowly decreasing part, which we associate with the damaged and fragmented regimes introduced above, respectively. We identify the transition point between the two states with the position of the maximum called *fragmentation threshold* η_c.

The separation of the two regimes and the identification of the transition point is also supported by the behavior of the mass of the largest fragment as a function of η. In Fig. 5 we present the sum of the mass of the largest fragments of the two bodies $M_{\max}=M^A_{\max}+M^B_{\max}$, normalized by the total mass $M_{\rm tot}=M^A+M^B$ versus η. The monotonically decreasing function has a distinct curvature change, the position of which, $\eta_c=0.36$, coincides with the maximum of the energy release curve ϵ_R. This also confirms that the behavior of the system sharply changes at a specific value of η that we call the fragmentation threshold η_c.

To clarify the influence of the overall size of the colliding bodies on the behavior of the fragmenting system, simulations were performed varying the radius R of the particles between 10 and 30 cm. Note that the average size of the randomly shaped unbreakable polygons is 1 cm. Figure 6 shows ϵ_R as a function of η for several values of R. It can be observed that the qualitative behavior of the curves is universal; it is independent of the system size, but the position of the transition point η_c is slightly shifted downward with increasing R.

IV. SIZE DISTRIBUTION OF FRAGMENTS

To reveal the nature of the transition from the damaged state to the fragmented state, the evolution of the fragment size distribution with varying impact energy is a crucial point. Since the dissipated energy E_R is proportional to the total surface of cracks, it is expected that the two regimes should clearly also show up in the type of disintegration of

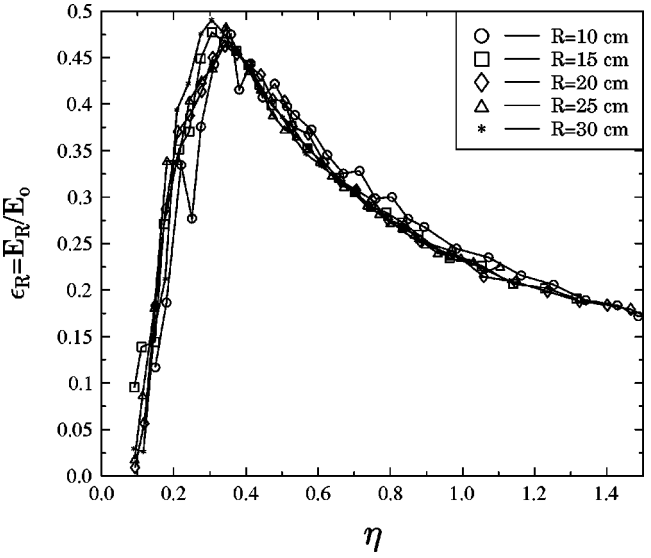

FIG. 6. The energy release curve ϵ_R at different system sizes R.

the solids, i.e., in the behavior of the size distribution of fragments. In the present section we demonstrate that, in the vicinity of η_c the behavior of the fragment size distribution shows strong similarities to that of the size distribution of clusters in systems undergoing a second order phase transition. As an example, one can mention the behavior of the cluster size distribution in percolation around the critical point p_c, or the size distribution of droplets in the vicinity of the critical temperature T_c in the case of the liquid-gas phase transition. Throughout this section we refer to percolation on finite lattices for the purpose of comparison.

The fragment mass histograms $F(m;\eta)$ corresponding to the colliding system of the preceding section are shown in Figs. 7(a) and 7(b) for several values of η below and above the transition point η_c. Here $F(m;\eta)$ denotes the number of fragments with mass m divided by the total number of fragments, averaged over ten collision events having the same η. In order to obtain the same statistics of the distribution at all sizes, a logarithmic binning was used, i.e., the binning is equidistant on logarithmic scale. The histograms have two cutoffs. The lower one is due to the existence of single unbreakable polygons, while the upper one is determined by the finite size of the bodies.

In Fig. 2 we have shown that a collision at η just above η_0 results in only a few small fragments and two large ones (with almost the same size), but no fragments are generated in the intermediate mass region. Hence, in Fig. 7(a) the corresponding mass distribution $F(m;\eta)$ has two peaks at small mass and large mass, with a large gap in between. Increasing η in Fig. 7(b), the main difference compared to Fig. 7(a) is that the peak of the large fragments gradually disappears; the large pieces break into smaller ones, giving rise to fragments in the intermediate mass region. For $\eta \to \eta_c$ the mass distribution $F(m;\eta)$ in the intermediate region tends to a power law:

$$F(m) \sim m^{-\tau}. \tag{4}$$

The value of the exponent obtained at $\eta = \eta_c$ is $\tau = 2.27 \pm 0.05$. Our former simulations showed (see Ref. [13]) that

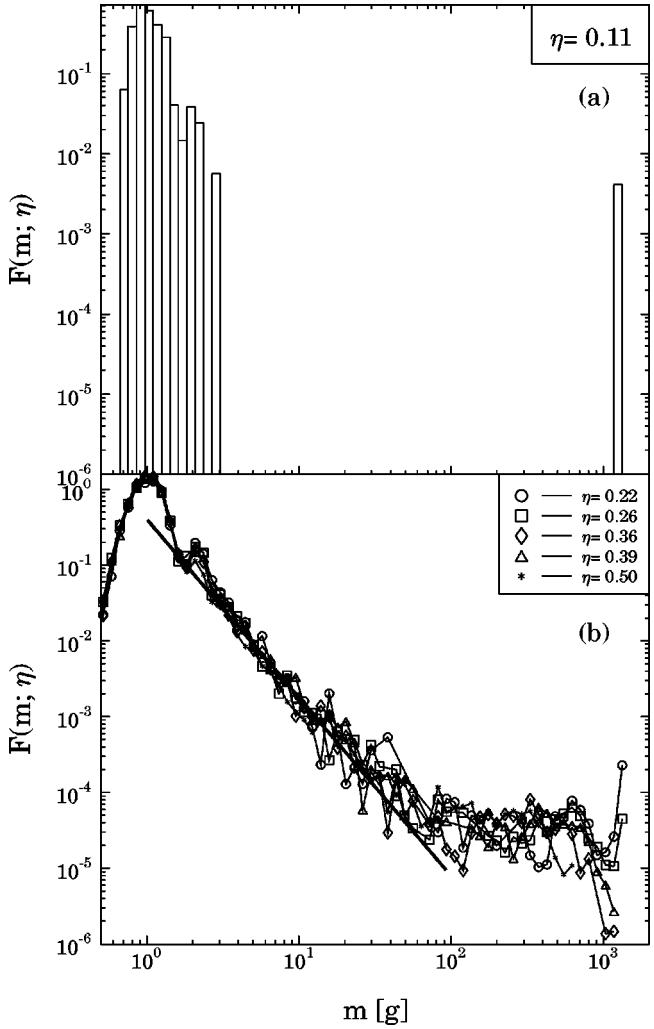

FIG. 7. Mass distribution of fragments at different values of η below and above the fragmentation threshold η_c. The peak of small fragments is due to the fact that single polygons are unbreakable in the model. The mass of the colliding disks with radius $R = 20$ cm was 1250 g.

the power law behavior of $F(m;\eta)$ remains valid for $\eta > \eta_c$, but the value of the exponent τ is a decreasing function of η, in agreement with most of the experimental observations [4–7].

To clarify the effect of the overall size of the colliding bodies R on the shape of the mass distribution $F(m;\eta)$ and on the value of the exponent τ, in Fig. 8 we plot the fragment size distributions at the transition point η_c for three different values of R. It can be seen that, upon increasing R, the power law region of $F(m;\eta_c)$ becomes wider and the relative height of the hump at large fragments decreases, but the value of the exponent τ does not change. It is important to note that in the case of percolation on finite lattices the size distribution of clusters shows the same shape and dependence on the system size at the critical point [30].

More insight into the evolution of the shape of $F(m;\eta)$ can be obtained by studying the moments of the distribution as a function of η. The kth moment $M_k(\eta)$ of the histogram $F(m;\eta)$ is defined as

$$M_k(\eta) = \sum_m m^k F(m;\eta). \tag{5}$$

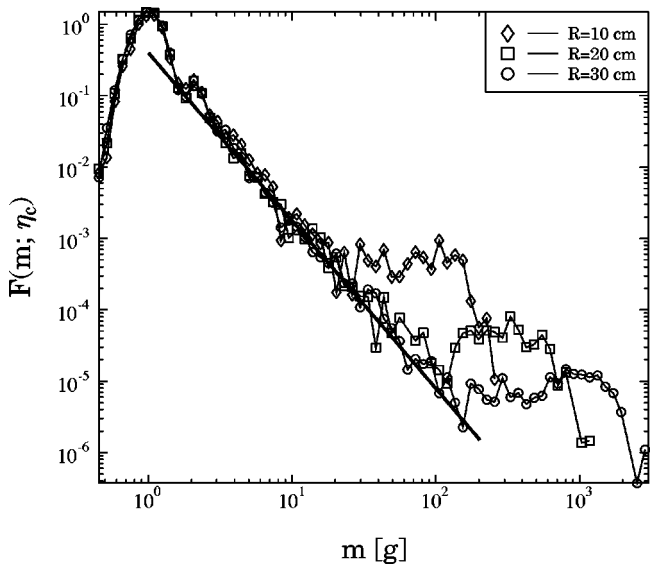

FIG. 8. Mass distribution of fragments at the transition point η_c for three different values of the system size R.

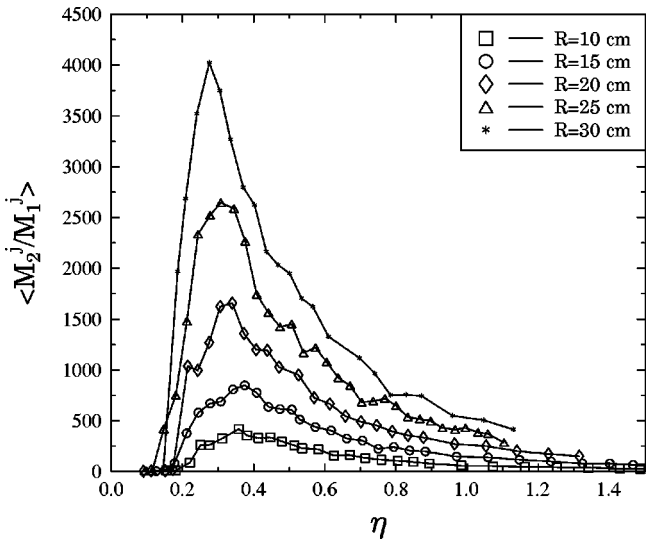

FIG. 9. $\langle M_2^j/M_1^j\rangle$ as a function of η for five different values of R.

In the case of critical phenomena like percolation or the liquid-gas transition, the moments M_k of the cluster size distribution with $k>1$ diverge at the critical point in the thermodynamic limit

$$M_k \sim |\epsilon|^{-\mu_k}, \tag{6}$$

where ϵ denotes the distance from the critical point, i.e., $\epsilon = p - p_c$ for percolation or $\epsilon = T - T_c$ for the liquid-gas transition. In a finite system the moments M_k have a finite maximum at the transition point. Assuming gap scaling for $F(m)$ [30],

$$F(m) \sim m^{-\tau} f(m^{\sigma}\epsilon), \tag{7}$$

the moment exponents μ_k can be expressed in terms of τ and σ,

$$\mu_k = \frac{1+k-\tau}{\sigma}, \tag{8}$$

and the behavior of the system in the vicinity of the transition point can be characterized by only two independent exponents τ and σ.

To test whether our small systems exhibit some trace of this behavior, we evaluated so-called *single event moments* M_k^j defined as

$$M_k^j = \sum_m{}' m^k n^j(m), \tag{9}$$

where the upper script j refers to the jth collision event, $n^j(m)$ denotes the number of fragments with mass m in event j, and the prime indicates that the sum runs over all the fragments excluding the largest ones of each of the two colliding bodies. The study of single event moments was first suggested by Campi and co-workers to reveal properties of fragmentation processes with varying imparted energy [31–33]. As demonstrated in Refs. [31–33], the usage of single event moments defined by Eq. (9) instead of Eq. (5) has the advantage that part of the analysis, e.g., the study of the correlation of moments in scatter plots, can be carried out without ordering the collision events according to a parameter like in our case η. Following Campi and co-workers's ideas, we evaluated the ratio of M_2^j and M_1^j

$$\frac{M_2^j}{M_1^j} = \frac{\Sigma_m' m^2 n^j(m)}{\Sigma_m' m n^j(m)} = \overline{M}^j, \tag{10}$$

which is equal to the average fragment size $\overline{M}^j$ in event j. $\langle M_2^j/M_1^j\rangle$ is plotted in Fig. 9 for several different values of the system size R as a function of η. The brackets $\langle\cdots\rangle$ denote that each data point was obtained as an average over ten events having the same η. One can observe that $\langle M_2^j/M_1^j\rangle$ has a distinct maximum, the position of which coincides with the maximum of the energy release curve ϵ_R in Fig. 6, within the precision of the calculations. It is very important to note that increasing the system size R the peak of $\langle M_2^j/M_1^j\rangle$ becomes sharper, i.e., the height of the peak increases while the width of the peak decreases, which is also typical for a critical point like the percolation threshold occurring in finite size systems [30,31,34].

The validity of gap scaling [Eq. (7)] for the mass distribution $F(m;\eta)$ can be easily tested by making scatter plots of moments M_k^j, i.e., by plotting M_k^j against $M_{k'}^j$ with $k,k'>1$, then checking the correlation of the moments and the validity of the relation of the exponents [Eq. (8)]. The scatter plot of two pairs of moments is shown in Fig. 10. For the purpose of normalization the moments with $k>1$ are divided by M_1^j. In Fig. 10 the collision events close to the transition point η_c are represented by points with the largest values of the moments. Events with η far below or far above η_c result in smaller values of M_k^j; hence the corresponding points in Fig. 10 fall closer to the origin. One of the most remarkable features of Fig. 10 is that the moments are strongly correlated in the region corresponding to the vicinity of the transition point η_c, and a power law seems to be a

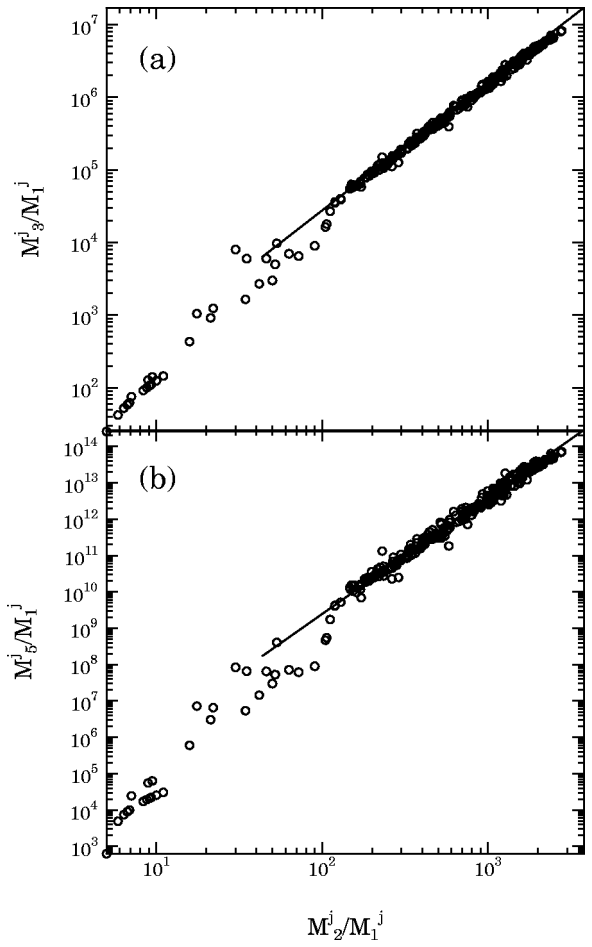

FIG. 10. Scatter plot of moments for the system of size $R=20$ cm. The straight lines were fitted to the data points in the range $M_2^j/M_1^j>300$.

reasonable fit to the scattered points. By this fitting procedure, one numerically obtains the ratio of the moment exponents μ_k and $\mu_{k'}$ since

$$M_k \sim M_{k'}^{\mu_k/\mu_{k'}}, \quad k,k'>1. \tag{11}$$

The value of the exponents obtained as the slope of the straight lines in Fig. 10 are $\mu_3/\mu_2=2.28\pm0.1$ and $\mu_5/\mu_2=4.95\pm0.17$, which are in agreement with the corresponding predictions 2.36 and 5.11, substituting $\tau=2.27$ into Eq. (8).

Hence we conclude that, within the limited precision available in our small system, the mass distribution of fragments fulfills the gap scaling relation [Eq. (7)], and the damage-fragmentation transition occurs as a continuous phase transition. The control parameter of the transition can be identified with the parameter η, and the quantity characterizing the size reduction $M_{\max}/M_{\text{tot}}$ can be considered as the order parameter. To complete the characterization of our system around η_c, we numerically determined the value of the order parameter exponent β defined as [35]

$$\frac{M_{\max}}{M_{\text{tot}}} \sim |\eta-\eta_c|^{\beta}, \quad \eta<\eta_c, \tag{12}$$

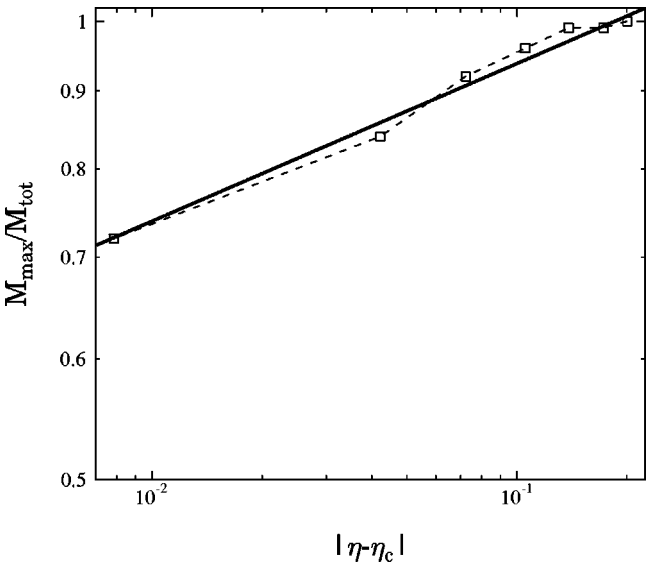

FIG. 11. Determination of the order parameter exponent β. The data of Fig. 5 are plotted here as a function of $|\eta-\eta_c|$ for $\eta<\eta_c$. The exponent β can be obtained as the slope of the least square fitted straight line.

and the value of the exponent γ characterizing the average fragment size:

$$\left\langle \frac{M_2^j}{M_1^j} \right\rangle \sim |\eta-\eta_c|^{-\gamma}. \tag{13}$$

The power law behavior given by Eq. (13) is valid on both sides of the critical point η_c. (Note that $\gamma=\mu_2$.) Using the data presented in Fig. 5, we plotted $M_{\max}/M_{\text{tot}}$ versus $|\eta-\eta_c|$ for $\eta<\eta_c$ in Fig. 11. It can be seen that a power law with an exponent $\beta=0.11\pm0.02$ gives a reasonable fit to the data. In Fig. 12, $\langle M_2^j/M_1^j\rangle$ belonging to the system size $R=20$ cm of Fig. 9 is depicted as a function of $|\eta-\eta_c|$ for $\eta>\eta_c$. Again a power law with an exponent $\gamma=0.26\pm0.02$ can be fitted with a reasonable quality. Since only two of the critical exponents are independent, we can check the consistency of our description by pairing the exponents τ,β, and γ and using the well known scaling laws [30,35] of critical phenomena to obtain the value of the other exponents. It can be observed in Table II that the numerical values of the exponents obtained by starting from the three possible pairs agree well with each other within the error bars, which gives further justification of our phase transition picture.

V. DISCUSSION

In the present paper we applied our dynamical model of granular solids to study impact fragmentation phenomena at low values of the imparted energy. Analyzing the energetics of the fragmentation process and the resulting size distribution of fragments, we identified two distinct final states of the impact process, i.e., *damaged* and *fragmented* states, with a sharp transition in between. With a detailed study of the behavior of the fragment mass distribution in the vicinity of the transition point and its dependence on the finite particle size we gave numerical evidence that the transition point

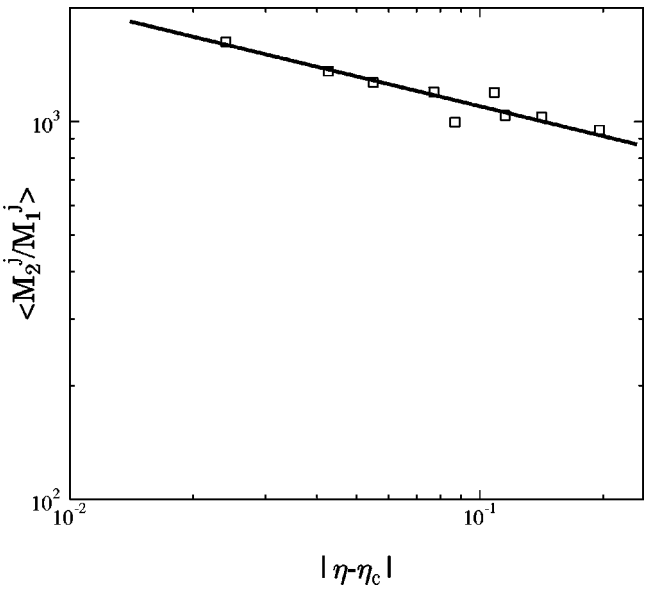

FIG. 12. To obtain the exponent γ we plotted $\langle M_2^j/M_1^j \rangle$ belonging to the system size $R=20$ cm of Fig. 9 as a function of $|\eta - \eta_c|$ for $\eta > \eta_c$. Data points are taken only from the vicinity of η_c. The exponent γ is obtained as the slope of the least square fitted straight line.

behaves as a critical point and that the *damage-fragmentation* transition occurs as a continuous phase transition. The control parameter of the transition was chosen to be the dimensionless ratio η of the energy of impact and the binding energy of the sample, and the order parameter was associated with the mass of the largest fragment divided by the total mass.

Based on the time evolution of the collision process obtained by the simulations, the following qualitative picture of the mechanism of the transition can be established: when two macroscopic solids collide, damage first occurs in the surroundings of the contact zone of the bodies. After this contact damage a compressive elastic pulse expands radially through the bodies, the amplitude of which strongly depends on the amount of primary damage that occurred in the contact zone. The pulse reflects back from the free boundary, and after reflection tensile forces arise in the solids, resulting in cracks in the bulk. The amount of breaking in the bulk is determined mainly by the amplitude of the initial pulse remaining after contact damage. The fragmentation of the colliding solids occurs above a specific value of the impact energy where the amplitude of the remaining pulse will be sufficient to give rise to a complete breakup of the bulk into pieces. At this specific energy value the behavior of the colliding system sharply changes, as we demonstrated by analyzing the energetics and the size distribution of fragments.

The idea of the existence of a so-called fragmentation phase transition was first addressed in the field of nuclear physics, where the fragmentation of heavy nuclei due to impact is extensively studied (for a recent review, see Ref. [36]). Using percolation based ideas it was shown that the disassembly of excited nuclei possesses a continuous phase transition when the imparted energy is varied [31–34]. The order parameter of the transition was associated with the size (charge) of the largest fragment.

Recently, the penetration of a steel ball into a solid plate with varying impact energy was studied experimentally [37]. It was reported that the so-called ballistic limit, i.e., the impact energy where the perforation of the plate occurs, behaves as a critical point, and the perforation occurs as a continuous phase transition, the order parameter of which was chosen to be the mass of ejecta expelled from behind the target. It was argued that the mechanism of the phase transition is the coalescence and percolation of randomly nucleated microcracks.

In an analysis of the numerical results obtained by a computer simulation of our dynamical model, we referred to the theory of percolation on finite lattices as an example of critical phenomena occurring in finite systems, without assuming percolation of microcracks. In this sense our analysis is free of model assumptions. In the snapshots of the final scenarios of collision processes it can be seen that the complicated elastic field arising due to propagation and interference of elastic waves gives rise to correlated crack growth. Hence, in our case, the assumption of percolation of cracks cannot be valid, and the values of the exponents obtained numerically are different from the corresponding exponents of percolation.

An important feature of our model which can affect the result of a fragmentation process is the existence of elementary, nonbreakable polygons, which hinders us from observing fragmentation on lower scales. In Ref. [15], using a discrete model of solids similar to ours, detailed tests of the

TABLE II. Test of the consistency of the critical exponents. Starting from the three possible pairs of τ, β, and γ, the value of the other exponents was derived using the scaling laws.

	(τ,β)	(τ,γ)	(β,γ)
β	0.11 ± 0.02	$\frac{\gamma(\tau-2)}{3-\tau} = 0.09 \pm 0.025$	0.11 ± 0.02
γ	$\frac{(3-\tau)\beta}{\tau-2} = 0.29 \pm 0.08$	0.26 ± 0.02	0.26 ± 0.02
σ	$\frac{\tau-2}{\beta} = 2.45 \pm 0.6$	$\frac{3-\tau}{\gamma} = 2.8 \pm 0.28$	$\frac{1}{\gamma+\beta} = 2.7 \pm 0.21$
τ	2.27 ± 0.05	2.27 ± 0.05	$2+\frac{\beta}{\gamma+\beta} = 2.3 \pm 0.04$
α	$2-\frac{(\tau-1)\beta}{\tau-2} = 1.48 \pm 0.12$	$2-\frac{(\tau-1)\gamma}{3-\tau} = 1.54 \pm 0.06$	$2-(2\beta+\gamma) = 1.52 \pm 0.045$

effect of the polygon size on the shape of the mass distribution of fragments in impact fragmentation were performed. It was found that if the tessellation of a solid is fine enough to reproduce the macroscopic elastic behavior correctly, the effect of the existence of unbreakable polygons on the size distribution of fragments occurs solely in the vicinity of the cutoff size, and the overall shape of the distribution is not affected. This also implies that the phase transition behavior revealed by our simulations is not influenced globally by the element size, but it can be expected that the critical regime becomes narrower when the element size decreases at a fixed value of the macroscopic size of the colliding bodies.

Studying kinetic models of fragmentation phenomena in Refs. [23,38] it was pointed out that under certain circumstances a so-called shattering transition might occur, when a macroscopic amount of mass of the fragmenting system is transformed into a dusty phase, i.e., into single polygons in our case. Since in discrete dynamical models such a shattering transition can occur only at very high impact energies, its investigation is not included in the present study.

The binary breakup of bond percolation clusters due to the removal of a single bond has also been studied in the context of fragmentation phenomena. The characteristic quantities describing the fragmentation of percolation clusters are the number of fragmenting bonds $a_s(p)$, i.e., the number of those bonds in the cluster of size s whose removal results in two disconnected clusters, and the probability $P_{s',s}(p)$ that the breakup of a cluster of size s results in a daughter cluster of size s' [39]. $a_s(p)$ and $P_{s',s}(p)$ are of fundamental interest because they describe the connectivity of percolation clusters, and they may also serve as inputs for the rate equations describing fragmentation processes as a sequence of binary events [23,38,39]. At the critical point $p=p_c$, both $a_s(p_c)$ and $P_{s',s}(p_c)$ show interesting scaling behaviors whose scaling exponents could be related to the critical exponents of percolation [39], but no phase transition was claimed in the breakup process. Although the form of $P_{s',s}(p_c)$ as a function of the daughter mass s' and its dependence on the global size of the fragmenting object s [39] is similar to some extent to the behavior of our fragment mass distribution at the critical point $F(m;\eta_c)$ (see Fig. 8), there is no direct analogy between the binary breakup of percolation clusters and our dynamic fragmentation process.

To our knowledge, no systematic experimental study of the transition from damage to fragmentation in impact of solids has been performed, so that we cannot confront the results of the simulations with experiments. For a deeper understanding of the transition predicted by our simulations, further experimental and more analytical theoretical studies are needed.

ACKNOWLEDGMENTS

F.K. is very grateful to R. Englman, Z. Jäger, and K. F. Pál for valuable discussions and for sending him reprints of their works on fragmentation. F.K. acknowledges financial support of the Alexander von Humboldt Foundation, and that of the Project Nos. SFB381 and OTKA T-023844.

[1] *Statistical Models for the Fracture of Disordered Media*, edited by H. J. Herrmann and S. Roux (North-Holland, Amsterdam, 1990).
[2] *Fragmentation Phenomena*, edited by D. Beysens, X. Campi, and E. Pefferkorn (World Scientific, Singapore, 1995).
[3] D. L. Turcotte, J. Geophys. Res. **91**, 1921 (1986).
[4] N. Arbiter, C. C. Harris, and G. A. Stamboltzis, Trans Soc. Min. Eng. AIME **244**, 118 (1969).
[5] T. Matsui, T. Waza, K. Kani, and S. Suzuki, J. Geophys. Res. **87**, 10 968 (1982).
[6] A. Fujiwara and A. Tsukamoto, Icarus **44**, 142 (1980).
[7] A. Fujiwara *et al.*, in *Asteroid II*, edited by R. P. Binzel, T. Gehrels, and M. S. Matthews (University of Arizona Press, Tucson, 1989).
[8] L. Oddershede, P. Dimon, and J. Bohr, Phys. Rev. Lett. **71**, 3107 (1993).
[9] A. Meibom and I. Balslev, Phys. Rev. Lett. **76**, 2492 (1996).
[10] H. Inaoka, E. Toyosawa, and H. Takayasu, Phys. Rev. Lett. **78**, 3455 (1997).
[11] T. Kadono, Phys. Rev. Lett. **78**, 1444 (1997).
[12] F. Kun and H. J. Herrmann, Comput. Methods Appl. Mech. Eng. **138**, 3 (1996).
[13] F. Kun and H. J. Herrmann, Int. J. Mod. Phys. C **7**, 837 (1996).
[14] A. V. Potapov, M. A. Hopkins, and C. S. Campbell, Int. J. Mod. Phys. C **6**, 371 (1995).
[15] A. V. Potapov, M. A. Hopkins, and C. S. Campbell, Int. J. Mod. Phys. C **6**, 399 (1995).
[16] C. Thornton, K. K. Yin, and M. J. Adams, J. Phys. D **29**, 424 (1996).
[17] W. Benz and E. Asphaug, Icarus **107**, 98 (1994).
[18] S. Steacy and C. Sammis, Nature **353**, 250 (1991).
[19] H. Inaoka and H. Takayasu, Physica A **229**, 1 (1996).
[20] M. Marsili and Y. C. Zhang, Phys. Rev. Lett. **77**, 3577 (1996).
[21] J. Åström and J. Timonen, Phys. Rev. Lett. **78**, 3677 (1997).
[22] J. Åström, M. Kellomäki, and J. Timonen, Phys. Rev. E **55**, 4757 (1997).
[23] R. Botet and M. Ploszajczak, Int. J. Mod. Phys. E **3**, 1033 (1994).
[24] R. Englman, J. Phys.: Condens. Matter **3**, 1019 (1991).
[25] G. Hernandez and H. J. Herrmann, Physica A **215**, 420 (1995).
[26] F. G. Bridges, A. Hatzes, and D. N. C. Lin, Nature (London) **309**, 333 (1984).
[27] H. J. Tillemans and H. J. Herrmann, Physica A **217**, 261 (1995).
[28] C. Moukarzel and H. J. Herrmann, J. Stat. Phys. **68**, 911 (1992).
[29] K. B. Lauritsen, H. Puhl, and H. J. Tillemans, Int. J. Mod. Phys. C **5**, 909 (1994).
[30] D. Stauffer and A. Aharony, *Introduction to Percolation Theory* (Taylor and Francis, London, 1992).
[31] X. Campi, J. Phys. A **19**, L917 (1986).
[32] X. Campi, Phys. Lett. B **208**, 351 (1988).
[33] X. Campi and H. Krivine, Z. Phys. A **344**, 81 (1992).
[34] W. Bauer, Phys. Rev. C **38**, 1297 (1988).

[35] N. Goldenfeld, *Lectures on Phase Transitions and the Renormalization Group* (Addison-Wesley, Reading, MA, 1992).

[36] J. S. Sá Martins and P. M. C. de Oliveira, Int. J. Mod. Phys. C **9**, 881 (1998).

[37] A. H. Mayer, Z. Jäger, and R. Englman (unpublished).

[38] S. Redner, in *Statistical Models for the Fracture of Disordered Media* (Ref. [1]).

[39] M. F. Gyure and B. F. Edwards, Phys. Rev. Lett. **68**, 2692 (1992); B. F. Edwards, M. F. Gyure, and M. Ferer, Phys. Rev. A **46**, 6252 (1992); J.-M. Debierre, Phys. Rev. Lett. **78**, 3145 (1997).